A Three-Dimensional Numerical Simulator for Microbial Enhanced Oil Recovery

G.V. Chilingarian[1] and M.R. Islam[2]

Microbial enhanced oil recovery (MEOR) is receiving renewed interest worldwide. MEOR involves the injection and transportation of microorganisms into the reservoir followed by nutrients which act as in situ growth products. These bacteria act as either a mobilizing agent of residual oil or a plugging agent for selective plugging of an undesired reservoir zone. Even though the concept of MEOR activities is rather straight-forward, field tests have often been dismal. One of the reasons for such failure has been reported to be the inability to set up proper field strategy. In order to develop a proper strategy, a reservoir simulator capable of predicting bacterial movement and reactions in an oil reservoir must be developed. Such a simulator has been nonexistent to date. This paper presents formulation and results of reservoir simulation using microbial EOR.

The formulation developed in this paper describes microbial transport in a multidimensional porous medium. This description is completed with a kinetic model of bacterial growth which leads to either bacterial plugging and mobility control or alteration of oil properties (reduction of oil viscosity; interfacial tension (IFT), etc.). Reservoir simulation results are given for different types of bacteria used. A Canadian heavy oil reservoir was used as the prototype for all numerical simulation results.

INTRODUCTION

The first suggestion for using MEOR was made as early as in 1926 [1]. The first detailed study of MEOR was conducted by ZoBell [2-4]. He observed that sulfate-reducing bacteria lead to gradual separation of oil or tar from the sand. The release of oil was explained through following phenomena:

- decomposition of inorganic carbonates,
- evolution of viscosity-reducing gases,
- IFT reduction due to bacterially produced surface-active substances.

Study in this area was further carried out by Beck [5] and Updegraff and Wren [6]. Ever since, there have been numerous research results reported in the literature. This has been recently summarized by Bryant and Burchfield [7].

Another aspect of MEOR deals with selective plugging of higher-permeability zones [8,9]. Jack and Doblasio [10] reported the use of slime-producing bacteria to selectively plug the high-permeability zones. In this process, the bacterial cells were injected in an unconsolidated porous pack. This was followed by the initiation of synthesis of extracellular slimes by a sucrose medium. Laboratory experiments

1. Department of Petroleum Eng., University of Southern California, L.A., CA, USA, 90089-1211.
2. Department of Geology and Geological Eng., South Dakota School of Mines and Technology, Rapid City, SD, USA, 57701-3995.

Scientia Iranica, Vol. 2, No. 1, © Sharif University of Technology, March 1995.

showed drastic reduction in permeability. This plugging technique was later tried in the field [11]. Even though the field test was a failure, it did give insight into the process and triggered much of the later research activities [12].

Even though there have been several studies reported in the areas of bacterial transport in porous media, little has been done for mathematical modeling of such a process. A simplified model was proposed by Knapp et al. [13]. This model used fundamental conservation laws along with growth and retention kinetics of biomass in order to predict porosity reduction as a function of distance and time. Updegraff [8] used a filtration model in order to express bacteria transport as a function of pore entrance size. A similar model was used by Jang et al. [14] as well. In a recent work, Jenneman et al. [9] modified the filtration theory to relate permeability with the rate of bacterial penetration. Some of these models were found to show good agreement with experimental results.

Unfortunately, all these models suffer from oversimplification and, more importantly, fail to differentiate surface filtration effects from transport through the porous medium in both the theory and the experiments. Also, none of these models incorporates fundamental laws of bacterial deposition or entrainment, or adsorption of bacteria to the rock surface. Only recently, Islam and Gianetto [15] reported a consistent numerical model for both microbial transport and the kinetics of bacterial growth. They also discussed the problem of scaling up of laboratory experiments conducted on MEOR processes. In this paper, this work is extended for field-scale reservoir simulation. Also, other aspects of MEOR, such as IFT reduction, mobility control and viscosity reduction are included in the mathematical description.

MATHEMATICAL FORMULATION

The mathematical formulation is written to describe multiphase multidimensional flow through porous media. The flow equations for oil, water and gas are as follows.

Water:

$$\left[\frac{kk_{rw}}{\mu_w B_w}\Phi_w\right] + q_w = \frac{\partial}{\partial t}\left[\phi\frac{S_w}{B_w}\right] . \tag{1}$$

Oil:

$$\left[\frac{kk_{ro}}{\mu_o B_o}\Phi_o\right] + q_o = \frac{\partial}{\partial t}\left[\phi\frac{S_o}{B_o}\right] . \tag{2}$$

Gas:

$$\left[\frac{kk_{rg}}{\mu_g B_g}\Phi_g + \frac{R_{sw}kk_{rw}}{\mu_w B_w}\Phi_w + \frac{R_{so}kk_{ro}}{\mu_w B_w}\Phi_o\right] + q_g + q_w R_{sw} + q_o R_{so} = \frac{\partial}{\partial t}\left[\phi\frac{R_{sw}S_w}{\mu_w B_w} + \phi\frac{R_{so}S_o}{\mu_o B_o} + \phi\frac{S_g}{B_g}\right] . \tag{3}$$

The bacterial transport is described by the following equation:

$$\left[\frac{C_{wb}kk_{rw}}{\mu_w B_w}\Phi_w\right] + q_w C_{wb} = \frac{\partial(\phi S_w \rho_w C_{wb} + \sigma)}{\partial t} . \tag{4}$$

The bacterial capture kinetics are given by Islam and Gianetto [15], following Gruesbeck and Collins [16] as:

$$\frac{\partial \sigma_{np}}{\partial t} = -\alpha(u_{np} - u_c)\sigma_{np} + \beta C , \tag{5}$$

$$\frac{\partial \sigma_p}{\partial t} = -(\delta + \rho\sigma_p)u_P C , \tag{6}$$

and

$$\phi_i \sigma = \phi_i f \sigma_p + (1 - f)\sigma_{np} , \tag{7}$$

where volumetric flux densities in the pluggable and nonpluggable pathways are related through respective permeabilities:

$$\frac{u_p}{u} = \frac{k_p(\sigma_p)}{k_p(\sigma_p) + k_{np}(\sigma_{np})} , \tag{8}$$

where u denotes volumetric flux density in any given direction. Permeability damage is

expressed through the following empirical relationship:

$$k_p \approx k_{pi} e^{-a\sigma_p^4} , \quad (9)$$

and

$$k_{np} \approx \frac{k_{npi}}{1 + \varepsilon\sigma_{np}} . \quad (10)$$

In the nutrient transport, there are several considerations. Very often, carbon and mineral sources are required to support the growth and metabolic activities of bacteria. There has been considerable evidence reported on adsorption taking place with sugar or protein nutrients in the presence of Berea Sandstone. Such adsorption is also expected in reservoir sands. Any adsorption model may be used to describe nutrient propagation through porous media. We chose the Langmuir equation for describing adsorption of a nutrient in porous media. In describing nutrient propagation through porous media, dispersion and diffusion are neglected. The nutrient transport equation appears as:

$$\left[\frac{C_{wn} k k_{rw}}{\mu_w B_w}\Phi_w\right] + q_w C_{wn} = \frac{\partial}{\partial t}\left[\phi\frac{S_w C_{wn}}{B_w}\right] + \frac{\rho_r}{\rho_w}(1-\phi)\frac{\partial C_{wn}}{\partial t} , \quad (11)$$

where the Langmuir equilibrium isotherm is written as:

$$c_r = \frac{a'C}{1 + bC} , \quad (12)$$

$$a' = \frac{K_1}{K_2} C_r^{\star} , \quad (13)$$

$$b = \frac{K_1}{K_2} . \quad (14)$$

When describing bacterial growth, one must look at several factors. The dependence of bacterial growth rate, μ, on nutrient concentration is represented by the Monod equation (Dawes and Sutherland, [17]):

$$\mu = \mu_m\left(\frac{C_{wn}}{K_S + C_{wn}}\right) , \quad (15)$$

where μ_m is the maximal growth rate obtained in excess nutrient, C_{wn} is the concentration of growth limiting substrate and K_S is the substrate concentration corresponding to half μ_m. In general, K_S, for most growth substrates, is very small. The values of μ_m and K_S used in this work are listed in Table 1. The μ_m value is taken from Dawes and Sutherland [17]. It is assumed that all other factors affecting growth rate, such as temperature and pH, remain constant.

Table 1. Reservoir model parameters.

Grid blocks in x-direction	20
Grid blocks in y-direction	20
Grid blocks in z-direction	10
Porosity	30%
Permeability, x-direction	5 μm^2
Permeability, y-direction	5 μm^2
Permeability, z-direction	1 μm^2
Oil viscosity	10 mPa.s
Water viscosity	1 mPa.s
Oil/water IFT	35 dynes/cm
S_{wi}	40%

It is assumed that the blocking of a porous channel takes place by exponential growth of bacteria. This is given by:

$$C_t = C_o\, e^{\mu t} , \quad (16)$$

where C_t is the concentration at time t and C_o is the initial concentration.

Reservoir simulation runs were conducted in order to simulate following cases:

1. Bacterial growth and plugging through biomass.
2. IFT-reducing surfactant generation.
3. Oil viscosity-reducing surfactant generation.
4. CO_2 generation.

Numerical Solution and Reservoir/Fluid Data

The flow equations were solved in a three-phase, three-dimensional framework. They

Table 2. Value of various parameters

K_s	0.1% wt
C_{ni}	5% wt
μ_m	1.3/hr
C_r^*	0.05 mg/g
α	1/cm
β	0.01/s
u_c	0.017 cm/s
δ	1/cm
ρ	1/cm
ε	1
a	1
K_p/K_{np}	10
f	0.2
C_{wbi}	0.1%wt

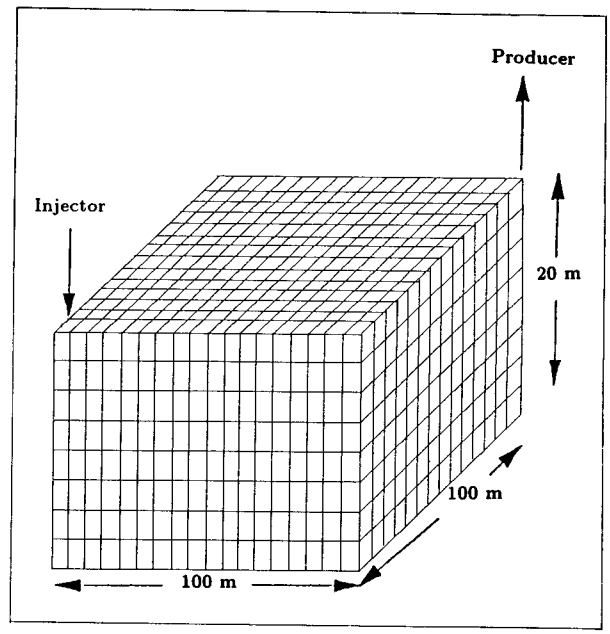

Figure 1. Grid blocks and injector/producer locations.

were solved following IMPES procedure. This was followed by the solution of the bacterial transport and nutrient transport equations. The bacterial transport equations were solved implicitly, whereas the nutrient transport equation was solved explicitly. This sequence was repeated until convergence for each time step. Note that the solution time was rather slow due to the changing permeability of the system. This was taken into account through changing relative permeability in order to avoid recalculating the constant part of the transmissibility equations. The oil/water relative permeability and capillary pressure curves were taken from Islam and Chakma [18]. Other reservoir parameters are given in Table 1. Parameters pertaining to bacterial transport and growth are given in Table 2. Figure 1 shows grid blocks and locations of injection and production wells in the reservoir.

RESULTS AND DISCUSSION

Bacterial Plugging

The first series of numerical simulations runs was conducted using single-phase fluid. Both injection and production rates were assumed to be 50 m^3 for all these cases. This was done to investigate the extent of bacterial plugging in a three-dimensional case. The use of single phase enabled one to compare overall permeability variation for different cases. Bacterial plugging may occur by two means:

1. Shear multiplication of the number of bacteria.
2. The generation of polymer in situ.

In the present work, we have modeled the first case following Islam and Gianetto [15]. However, the modeling is extended to three dimensions and to reservoir scale. Results of reservoir modeling (both for three- and one-dimensional cases) are compared with that predicted on a linear core. The linear core results are essentially the same as those reported by Islam and Gianetto [15]. These results are extrapolated on the basis of pore volumes of fluid injected. Figure 2 shows this comparison. All these runs are conducted assuming 20% pore volume of bacteria injection, followed by nutrient injection and then by chase water. First, note the difference between the results of one-dimensional and three-dimensional modeling. All parameters, except dimensionality,

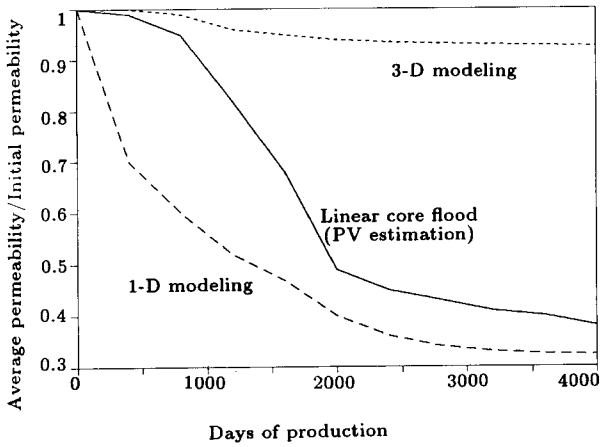

Figure 2. Comparison of permeability reduction due to bacteria injection.

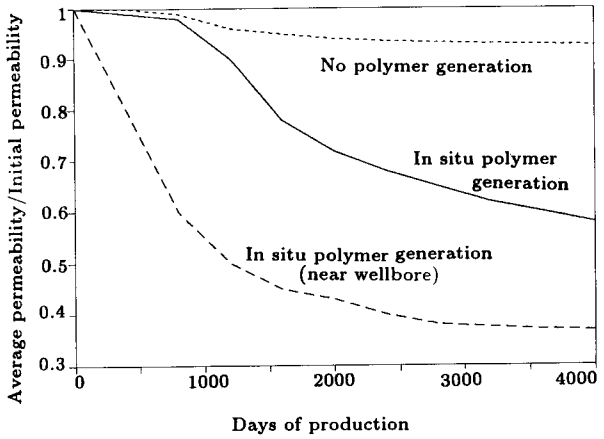

Figure 3. Comparison of permeability reduction due to bacteria injection and polymer generation.

were kept constant for these two cases. In a one-dimensional analysis, the bacterial plugging occurs quickly in the first block and reduces permeability to such an extent that further fluid injection leads to continuing bacterial build-up in the first few blocks. This reduces overall permeability drastically. Obviously, the field problem is not a one-dimensional one.

In three-dimensional modeling, the problem of local plugging is overcome and overall permeability reduction is much lower than what is obtained by one-dimensional modeling. Also, three-dimensional modeling correctly tracks the path of nutrients, which do not necessarily follow that of the bacteria. A deviation between these two paths may be only allowed through three-dimensional modeling. Comparison of these results with linear core flood results reflect the importance of time scaling in a laboratory study. Since laboratory experiments are conducted for a much shorter time, time-dependent variables (especially those related to bacterial growth) behave differently. The residence time being short, plugging is not shown as being as intense as in the one-dimensional model predictions. This analysis shows the importance of scaling time-dependent groups as outlined by Islam and Gianetto [15].

The effect of in situ polymer generation is modeled simply by using higher growth rate of bacteria. Figure 3 shows the effect of $\mu_m = 6.5/\text{hr}$ on permeability loss. As can be seen from this figure, substantial permeability loss is observed for this case. This effect is more intense for the near wellbore permeability reduction. Near wellbore is considered to be three blocks surrounding the injection block. A low near-wellbore permeability may lead to injectivity problem in a field situation. A more rigorous treatment of in situ polymer generation could be done if enough experimental data were available to define the flow and kinetic parameters involved in the process.

The effect of slug size of bacteria solution on permeability reduction for the case of polymer generation is shown in Figure 4. Note that all these results were obtained using three-dimensional modeling. A 5% slug does not

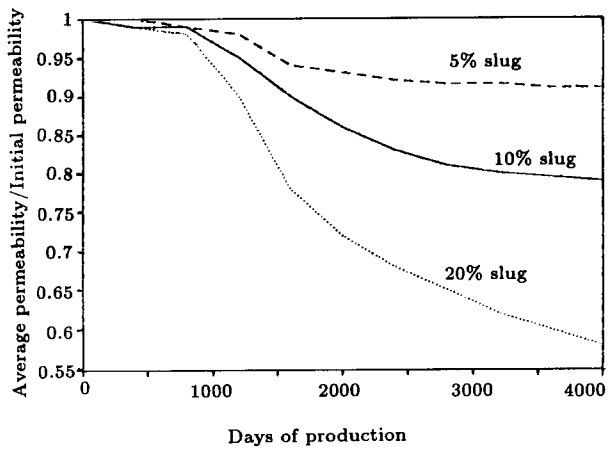

Figure 4. Effect of slug size on permeability reduction due to polymer generation.

appear to give any appreciable permeability reduction. In a three-dimensional case, 5% bacteria solution leads to a relatively small surface area to be in contact with the nutrient solution, which follows the bacteria. Consequently, nutrients find only a limited amount of bacteria in order to trigger bacterial growth and consequent plugging. This is followed by chase water, which simply washes away much of the nutrients, and bacteria stop growing, leading to minimal permeability reduction for this case.

IFT Reduction with Bacteria

In order to model bacteria-generated surfactant flood, it is assumed that interfacial tension (IFT) is a function of bacteria concentration. Figure 5 shows the IFT vs bacteria concentration curve which is used in this paper. Due to the lack of experimental data, such a curve was estimated from surfactant-flood type data. Also, following Bang and Caudle [19], the relative permeability curves were related to the IFT values in the following manner:

$$k_{ro} = k_{ro}(S_o) + [S_o - k_{ro}]\frac{\sigma_{max} - \sigma(C_b)}{\sigma_{max}}, \quad (17)$$

$$k_{rw} = k_{rw}(S_w) + [S_w - k_{rw}]\frac{\sigma_{max} - \sigma(C_b)}{\sigma_{max}}. \quad (18)$$

In this formulation, it is assumed that the relative permeabilities to water and oil are straight lines (extending from 0 to 1) when the IFT, σ, is zero. As the IFT approaches 0, these relative permeability curves approach straight line forms. Also, the following capillary pressure curves were used in order to incorporate dependence of the capillary pressure on $\sigma(C_b)$:

$$p_c[\sigma(C_b)] = p_1 p_c(\sigma_{max}, S_w).[\sigma(C_b)/\sigma_{max}], \quad (19)$$

where p_c becomes 0 if σ is 0.

Initial reservoir conditions and saturations are given in Table 1. In order to compare results, a base case of waterflooding was carried out. Similar to the field practice, surfactant-generating bacteria were injected following waterflooding when the oil cut was less than 5%. Such a low oil cut was obtained after 2400 days, at which time bacteria injection was initiated. In order to minimize the effect of bacterial plugging, the deposition rate was assumed to be 0.002/cm, a value 5 times smaller than that of the plugging bacteria. The injection rate was kept constant at 50 m^3/day for all the cases. The production well was operated at a total production constraint of 50 m^3/day. For this case, a 20% pore volume of bacteria solution was injected. This was followed by nutrient injection. Unlike the plugging case, nutrient injection was carried out throughout the final phase of the water injection. This ensured bacterial growth and surfactant generation in an uninterrupted fashion. Results of waterflood and bacteria injection are compared in Figure 6. Note that there is no improvement with bacteria for over 300 days of injection. This delay is expected, since bacteria concentration has to increase substantially away from the

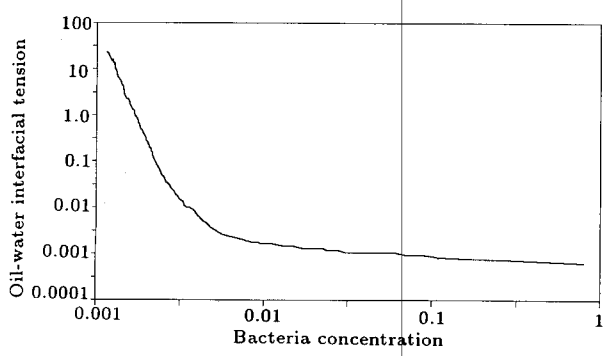

Figure 5. Correlation of bacteria concentration vs. oil-water interfacial tension.

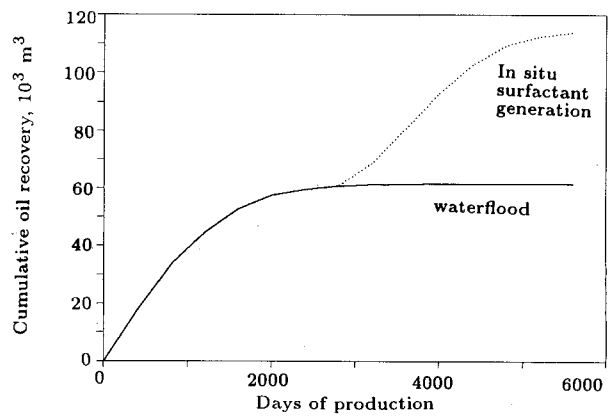

Figure 6. Comparison of oil recovery between bacteria-generated surfactant flood and waterflood.

injection well to mobilize oil near the production wellbore. However, as the oil mobilization takes place, oil cut increases rapidly. This leads to an incremental oil recovery of some 50.10^3 m^3. This is an improvement of 80% over a conventional waterflood. Whereas the exact amount of incremental oil recovered will depend largely on the nature of the IFT vs bacteria concentration, this exercise clearly shows that surfactant-producing bacteria can be used as an improved waterflooding technique.

A final run for surfactant-generating bacteria was conducted in a huff and puff mode. Only one well was used for this particular run. Bacteria was injected at a rate of 50 m^3/day for 10 days, followed by nutrient injection at 50 m^3/day for 10 days. Following this, the well was closed for 20 days prior to production. Similar to the previous case, post waterflood conditions were used as the initial conditions for the bacteria injection. The first cycle gave an average oil cut of 60% for 20 days for a total of 600 m^3 of oil. Several cycles of the operation were conducted. As the process progressed, the oil cut decreased gradually. After 5 cycles, a total of 14,500 m^3 of oil was produced. This result is shown in Figure 7. These results indicate that even though huff and puff has much quicker response time than does the drive process, total incremental oil recovery is considerably smaller for this case. However, a huff and puff scheme may be optimized by better planning of shut-in and production times. This was not done in the present study.

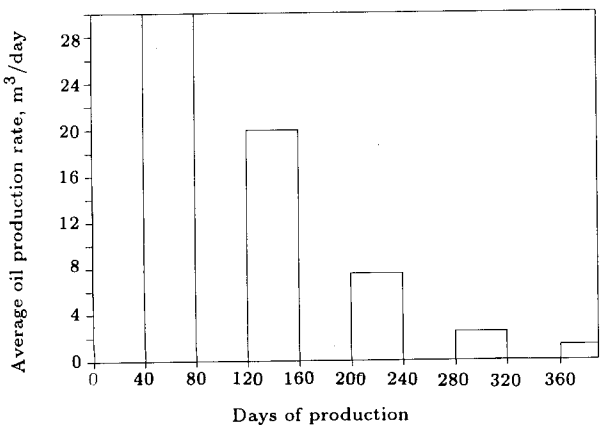

Figure 7. Oil flow rates of huff and puff with bacteria-generated surfactant.

Viscosity-Reducing Bacteria

An oil viscosity of 50 mPa.s was used for this study. This viscosity can be decreased considerably in the presence of bacteria. However, no conclusive experiment has been conducted to find out how oil viscosity correlates with bacterial concentrations. By analogy to solvent flood, a μ_o vs bacteria concentration curve, as in Figure 8, is proposed for the present study. An improved prediction may be done by providing experimental curves for μ_o vs bacterial concentration.

Figure 9 compares recovery results of viscosity-reducing bacteria with that of waterflooding. Note that the main difference

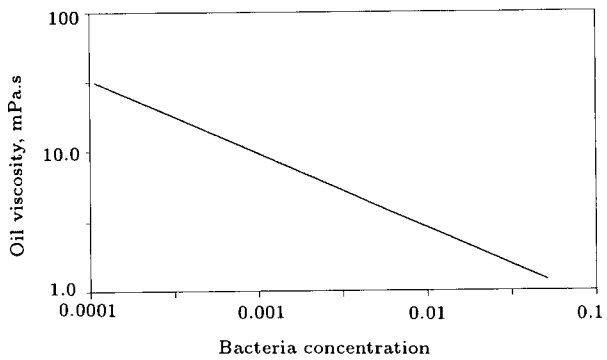

Figure 8. Correlation of oil viscosity vs bacteria concentration.

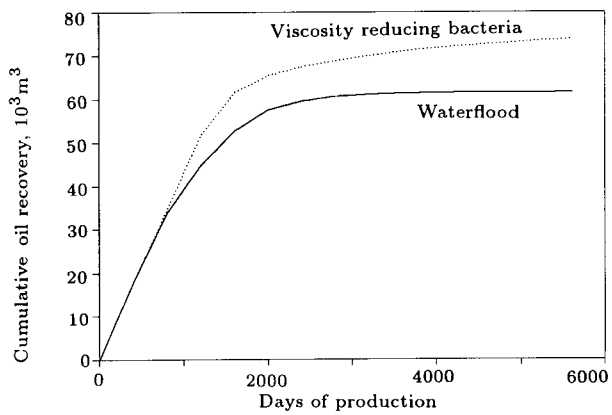

Figure 9. Comparison of oil recovery between viscosity-reducing bacterial injection and waterflood.

between the two curves is the delay in water breakthrough for the case of bacteria injection. Following water breakthrough, oil recovery declines in a way similar to the waterflood case. However, during this process, close to 15,000 m^3 of additional oil is recovered. This improvement is much less than that shown during bacteria-generated surfactant flood. Even though this is an indication that decreasing IFT is a better way to recover residual oil, no quantitative conclusion may be made from this study. Two factors of uncertainty are involved here. The first factor is that the nature of IFT reduction or oil viscosity reduction are not known. The second factor is that the presence of moderately viscous oil limits the benefit of oil viscosity reduction. It would probably be more appropriate to compare results with very high-viscosity oil for which a drastic decrease in oil viscosity would lead to great improvement over a waterflood.

CO_2-Generating Bacteria

The final run was conducted to simulate performance of CO_2-generating bacteria. Three-phase relative permeabilities were deduced by using Stone's method. Gas-oil relative permeability was taken from Islam et al. [20] who reported CO_2-heavy oil relative permeabilities obtained by history matching experimental results.

Once again a correlation between bacteria concentration and CO_2 volume was assumed. Figure 10 shows such a correlation. Such a correlation is not available in the literature and, therefore, an arbitrary curve had to be used. The nature of this curve will determine the oil recovery performance.

CO_2 generation was simulated by a source term in each block where the bacteria concentration is higher than 0.0001. In order to eliminate the numerical problem of appearance of gas-phase, a continuous gas phase was assumed to be existent in the reservoir (at 15%). A R_s value of 50 m^3/m^3 was used throughout. This value is reasonable for heavy oil reservoirs at 300 psi as in the present case.

Oil viscosity reduction and IFT reduction due to the presence of CO_2 was considered following Islam et al. [21]. Figure 11 compares results of CO_2 generation with waterflooding. Note that bacteria injection was carried out for 20% pore volume of the slug and was followed by continuous nutrient injection. This led to increasing bacteria population and the generation of a large amount of CO_2. However, as Figure 11 shows, results of CO_2 generation was not very encouraging. It appears that while CO_2 is beneficial for pressurizing the reservoir, it is detrimental to oil flow, much of which is restricted by the presence of a third phase. This can be shown by simple analysis of Stone's method. In this regard, changing the correlation of Figure 10 would not make much of a difference. In any case, the bacteria-generated CO_2 appears to recover as much oil as an immiscible CO_2 and water would. In our estimation, unless CO_2 reduces

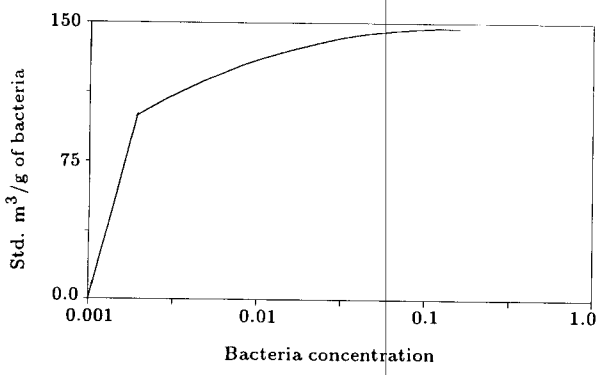

Figure 10. Correlation of CO_2 generation vs bacterial concentration.

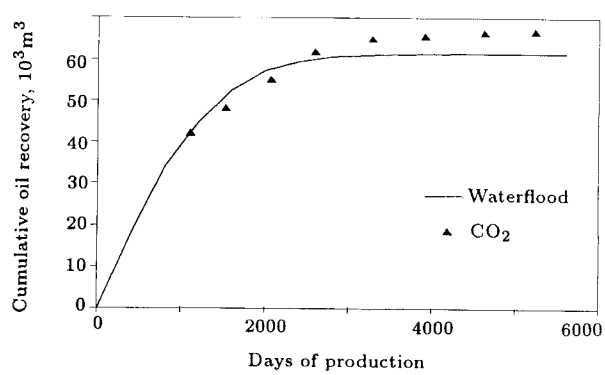

Figure 11. Comparison of bacterial generated CO_2 injection and waterflood.

oil viscosity to a considerably lower value, CO_2-generating bacteria do not hold much promise for recovering additional oil.

CONCLUSIONS

A reservoir simulator, complete with bacterial transport model and kinetics of bacterial growth, has been developed. Comparisons are made for one-dimensional and three-dimensional modeling of bacterial plugging. Conventional scaling up of laboratory data or modeling a three-dimensional problem with a one-dimensional model is likely to give erroneous results. Comparisons are made between various microbial enhanced oil recovery schemes and a base waterflood case. Surfactant-generating bacteria appear to be the most promising. However, more experimental data are needed before a conclusive remark can be made.

NOMENCLATURE

a	dimensionless constant
B	formation volume factor
C	concentration
$C_r^\star$	maximum obsorptive capacity of the rock
f	fraction of pore space containing pluggable pathways
g	acceleration due to gravity
k	absolute permeability
k_1	kinematic constant for absorption
k_2	kinematic constant for desportion
k_{ri}	relative permeability to phase i
o	potential of the phase i
p_i	pressure in phase i
q_i	injection rate of phase i
R_{si}	solution gas ratio for phase i
S_i	saturation to phase i
t	time
u	volume flux density
u_c	critical volume flux density
α	constant, 1/cm
β	constant, 1/s
δ	constant, 1/cm
ε	dimensionless constant
μ_i	viscosity of phase i
μ	bacterial growth rate
μ_m	maximal bacterial growth rate
ρ	constant, 1/cm
ρ_i	density of phase i
σ	volume of fines deposited per unit initial pore volume
ϕ	porosity

Subscripts

b	bacterial
c	critical value
i	initial conditions
n	nutrient
o	oil phase
np	nonplugging pathways
p	plugging pathways
t	temporal
w	aqueous phase

REFERENCES

1. Beckmann, J.W. "The action of bacteria on mineral oil", *Ind. Eng. Chem. News*, **4**, p 3 (1926).
2. ZoBell, C.E. "The effect of solid surfaces upon bacterial activity", *J. Bact.*, **46**, pp 39–56 (1943).
3. ZoBell, C.E. "Bacterial release of oil from oil-bearing materials (part I)", *World Oil*, **126**(13), pp 36–47 (1947).
4. ZoBell, C.E. "Bacterial release of oil from sedimentary materials", *Oil & Gas J.*, **46** (13), pp 62–65 (1974).
5. Beck, J.V. "Penn grade progress on use of bacteria for releasing oil from sands", *Producers Monthly*, pp 13–19 (Sept. 1947).

6. Updegraff, D.M. and Wren, G.B. "The release of oil from petroleum-bearing materials by sulfate-reducing bacteria", *Appl. Microbiol.*, **2**, pp 309–322 (1954).

7. Bryant, R.S. and Burchfield, T.E. "Review of microbial technology for improving oil recovery", *SPE Res. Eng.*, pp 151–154 (May 1989).

8. Updegraff, D.M. "Plugging and penetration of petroleum reservoir rock by microorganisms", *Proc. Int. Conf. on Microbial Enhanced Oil Recovery*, Afton, OK, pp 80–85 (1982).

9. Jenneman, G.E., Knapp, R.M., Menzie, D.E., McInerney, M.J., Revus, D.E., Clark, J.B. and Munnecke, D.M. "Transport phenomena and plugging in Berea Sandstone using microorganisms", *Proc. Int. Conf. on Microbial Enhanced Oil Recovery*, Afton, OK, pp 71–75 (1982).

10. Jack, T.R. and Doblasio, E. "Selective plugging for heavy oil recovery", *Microbes and Oil Recovery*, **1**, *Int. Bioresources J.*, Zajic and Donaldson, Eds., pp 205–212 (1985).

11. Stehmeier, L., Jack, T.R., Blakely, B.A. and Campbell, J.M. "Field test of a microbial plugging system at Standard Hill, Saskatchewan to inhibit oil field water encroachment", presented at the Biohydro Metallurgical Conference, Jackson Hole, WY, USA (Aug. 1989).

12. Jack, T.R., Stehmeier, L., Ferris, G. and Islam, M.R. "Microbial selective plugging to control water channeling", *Microbial Enhancement of Oil Recovery - Recent Advances*, E.C. Donaldson, Ed., Elsevier Science Publishers, Amesterdam Netherlands (1990).

13. Knapp, R.M., McInerney, M.J., Menzie, D.E. and Jennemen, G.E. "The use of microorganisms in enhanced oil recovery", Status Report of U.S. DOE Contract (1982).

14. Jang, K.L., Sharma, M.M., Findley, J.E., Chang, P.W. and Yen, T.F. "An investigation of the transport of bacteria through porous media", *Proc. Int. Conf. on Microbial Enhanced Oil Recovery*, Afton, OK, pp 60–70 (1982).

15. Islam, M.R. and Gianetto, A. "Mathematical modeling and scaling up of microbial enhanced oil recovery", *J. Can. Pet. Tech.*, pp 30–36 (April 1993).

16. Gruesbeck, C. and Collins, R.E. "Entrainmental deposition of fine particles in porous media", *Soc. Pet. Eng. J.*, pp 847–856 (Dec. 1982).

17. Dawes, I.W. and Sutherland, I.W. *Microbial Physiology*, Blackwell Scientific Publications, Oxford, London, UK (1976).

18. Islam, M.R. and Chakma, A. "Mathematical modeling of enhanced oil recovery by alkali solutions in the presence of cosurfactant and polymer", *J. Pet. Eng. Sci.*, **5**, pp 105-126 (1991).

19. Bang, H.W. and Caudle, B.H. "Modeling of a micellar/polymer process", *Soc. Pet. Eng. J.*, **24**, pp 617-627 (1984).

20. Islam, M.R., Erno, B.P. and Davis, D. "Hot gas and waterflood equivalence of in situ combustion", *J. Can. Pet. Tech.*, pp 44-52 (Oct. 1992).

21. Islam, M.R., Chakma, A. and Jha, K. "Heavy oil recovery by inert gas injection with horizontal wells", *J. Pet. Sci. Eng.*, **11**(3), pp 213-226 (1994).